



Application of Transfer Learning and Ensemble Learning in Image-level Classification for Breast Histopathology

Yuchao Zheng^a, Chen Li^a, Xiaomin Zhou^a, Haoyuan Chen^a, Hao Xu^a, Yixin Li^a, Haiqing Zhang^a, Xiaoyan Li^b, Hongzan Sun^b, Xinyu Huang^c, Marcin Grzegorzec^c

^aMicroscopic Image and Medical Image Analysis Group, College of Medicine and Biological Information Engineering, Northeastern University, Shenyang, China

^bChina Medical University, Shenyang, China

^cInstitute of Medical Informatics, University of Luebeck, Luebeck, Germany

Abstract

Background: Breast cancer has the highest prevalence in women globally. The classification and diagnosis of breast cancer and its histopathological images have always been a hot spot of clinical concern. In Computer-Aided Diagnosis (CAD), traditional classification models mostly use a single network to extract features, which has significant limitations. On the other hand, many networks are trained and optimized on patient-level datasets, ignoring the application of lower-level data labels.

Method: This paper proposes a deep ensemble model based on image-level labels for the binary classification of benign and malignant lesions of breast histopathological images. First, the BreaKHis dataset is randomly divided into a training, validation and test set. Then, data augmentation techniques are used to balance the number of benign and malignant samples. Thirdly, considering the performance of transfer learning and the complementarity between each network, VGG16, Xception, ResNet50, DenseNet201 are selected as the base classifiers.

Result: In the ensemble network model with accuracy as the weight, the image-level binary classification achieves an accuracy of 98.90%. In order to verify the capabilities of our method, the latest Transformer and Multilayer Perception (MLP) models have been experimentally compared on the same dataset. Our model wins with a 5% – 20% advantage, emphasizing the ensemble model's far-reaching significance in classification tasks.

Conclusion: This research focuses on improving the model's classification performance with an ensemble algorithm. Transfer learning plays an essential role in small datasets, improving training speed and accuracy. Our model has outperformed many existing approaches in accuracy, providing a method for the field of auxiliary medical diagnosis.

© 2022 Published by Elsevier Ltd.

Keywords: Convolutional Neural Network, Transfer Learning, Ensemble Learning, Image Classification, Histopathological Image, Breast Cancer

1. Introduction

Breast cancer is one of the most common malignant epithelial tumors in the world. According to the latest statistics from the International Agency for Research on Cancer (IARC) of the World Health Organization (WHO), there are 2.26 million new cases of breast cancer worldwide, surpassing the 2.2 million cases of lung cancer. At the end of

Email address: lichen201096@hotmail.com (Chen Li)

2020, breast cancer officially replaced lung cancer and became the world’s largest cancer [1]. Early treatment of breast cancer is vital, and doctors need to choose an effective treatment plan based on its malignancy. Therefore, the detection of breast cancer, the distinction between cancerous structure and the identification of its malignant degree is valuable. Previously, there were many techniques for detecting breast cancer, including Magnetic Resonance Imaging (MRI) [2], Computed Tomography (CT), Positron Emission Tomography (PET) [3], Ultrasound technology (US) [4], Mammograms (X-ray) [5] and Breast Temperature Measurement [6], etc.

At present, histopathological diagnosis is generally regarded as a “gold standard” [7]. Pathologists need to observe the tissue lesions under the microscope to determine the cancerous area and the degree of malignancy based on tissue structure, the nucleus and cytoplasm, and the growth pattern of the cells. To better analyze the different components of the tissue under the microscope, histopathologists usually stain the cut tissue. In all staining methods, Hematoxylin and Eosin staining has been frequently used for more than a hundred years, abbreviated as H&E [8]. Fig. 1 shows images of different types of breast tissues stained with H&E. Blue is the color of cell nuclei in excised tissues stained with hematoxylin, and pink is the color of other structures (cytoplasm, matrix, etc.) stained with eosin. According to their biological behaviors, breast lesions can be divided into benign lesions (Fig. 1 (b)) and malignant lesions (Fig. 1 (c)(d)). Benign lesions generally grow slowly and do not exhibit an invasive growth pattern, while malignant tumor tends to metastasize to lymph nodes and distant organs.

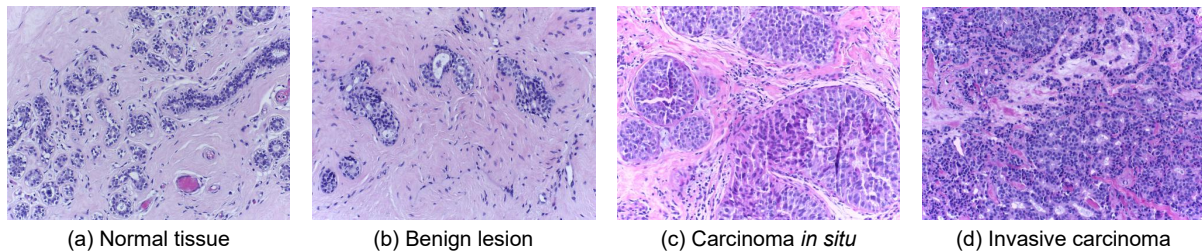


Figure 1. Breast tissue types based on H&E staining.

However, it is tough for a histopathologist to observe the tissue with the naked eyes and manually analyze the visual information based on prior medical knowledge. For one thing, manual analysis takes much time. The histopathological image itself will lead to complexity and diversity due to subtle differences, cell overlap, uneven color distribution and others. For another, the objectivity of this kind of analysis is unstable. The reason is that it depends largely on the experience, workload, and emotion of the histopathologist [9]. Authoritative pathologists still need highly professional training and rich experience to make a reliable diagnosis of patients, but the expertise and experience are also quite hard to inherit or innovate. Therefore, there is an urgent need for a system that can realize *Breast Histopathology Image Classification* (BHIC) to distinguish between cancerous tissue (malignant tissue) and non-cancerous tissue (benign tissue) to help pathologists make the diagnosis process more efficient and straightforward.

With the enhancement of computer calculating capacity and the continuous improvement of storage performance, CAD technology has quickly become an indispensable technology in the medical field, especially in the realm of histopathological image analysis. Currently, the medical reliance on CAD systems has increased year by year. The histopathological images can be quickly filtered and pre-classified by the CAD system, and then clinical doctors can obtain the second idea of early diagnosis. This helps reduce the burden on pathologists and improves the efficiency of work. Meanwhile, it can also concentrate the influence of pathologists on subjectivity and personal experience differences. With the assistance of application technology in the CAD system, the difference between observers has been further avoided. Above all, It is a work with research significance and broad application prospects.

Faced with this situation, much research around the world is ongoing. However, most of the existing methods are based on a single classifier. On the other hand, very few classification models based on image-level can achieve good classification results. This is because image-level classification is more complex: Images under the same patient-level label are related, making it easier to obtain better classification results; in contrast, image-level images only have relatively independent labels, and there is no correlation between each label and less practical information than patient-level images. While patient-level images are of great value in medical diagnosis, they sometimes add to the

problem. For example, in the Medical Image Retrieval System [10], when the doctor encounters a difficult disease, a query image can be sent to the system for assisted diagnosis through the retrieval system. It is very inconvenient to upload full slices or a whole set of data, and image-level data can greatly simplify upload, so image-level analysis is also very valuable. Therefore, this paper proposes an image-level classification method based on transfer learning and ensemble learning. It is believed that based on the original research, ensemble learning and transfer learning can provide users with easy-to-operate software and achieve better classification results. Since transfer learning utilizes a pre-trained model, it can significantly adapt to a small dataset in a short time [11]. Ensemble learning can complement the advantages of multiple networks, significantly improving the accuracy and generalization ability of the model. At the same time, compared with the classification task under the patient-level label, the classification of the lower image-level is more challenging. The workflow is shown in Fig. 2.

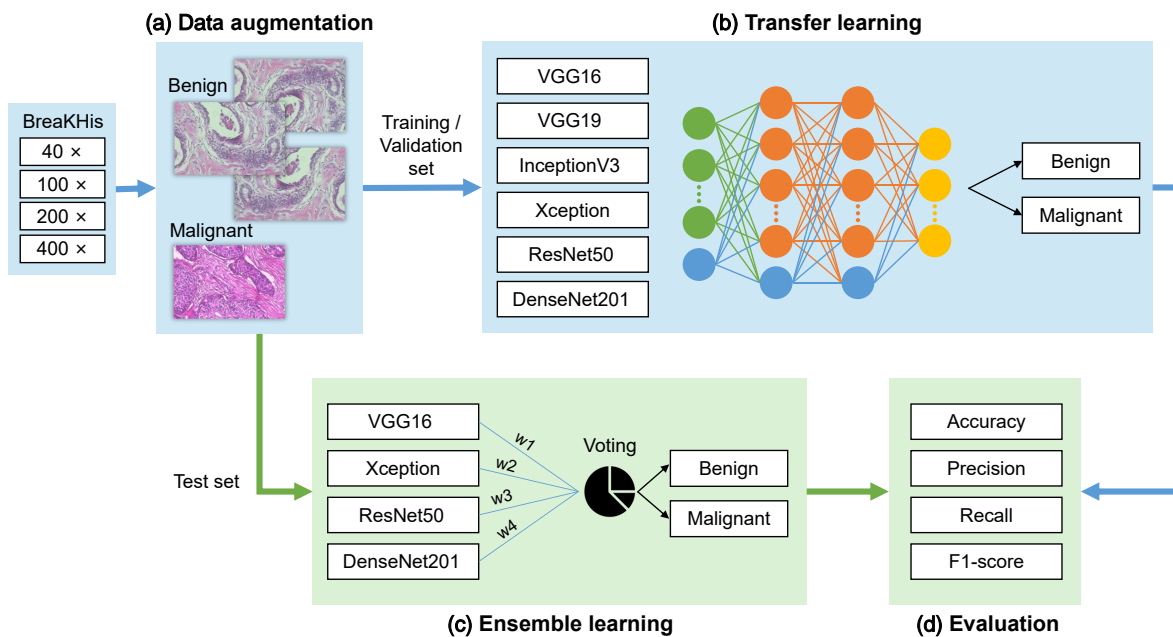


Figure 2. Workflow of the proposed work.

As the workflow presented, the basic framework of this method is mainly composed of four parts:

(a) Data augmentation. All of the images from the BrecaKHis dataset are divided into training, validation and test sets at the ratio of 7:1:2. Then the benign images are augmented through mirror flipping in order to balance the benign and malignant sample quantities.

(b) Transfer learning. The convolutional neural networks (CNNs), including VGG16, VGG19, ResNet50, InceptionV3, Xception and DenseNet201 are used for transfer learning to get applicable networks. According to the evaluation indicators, four out of six models are chosen as the base classifiers for the next process.

(c) Ensemble learning. This strategy based on the weighted voting method is used to further improve the classification performance. And the accuracy, one of the evaluation indicators, is chosen as the weight.

(d) Evaluation. The accuracy, precision, recall and F1-score are used as indicators to measure the classification ability of the whole algorithm.

The main contributions of this study are summarized as follows:

(1). This subject has technical advantages. A new framework is proposed to solve the classification problem of breast cancer histopathological images. In our previous work [12], the application of classic neural networks and deep learning in breast tissue pathological images from 2012 to early 2020 has been summarized in detail. At the same time, combined with the analysis of the literature in recent years, it is found that there are not many ideas for adopting the method of ensemble learning, which is very promising for research.

(2). Sufficient experiments are guaranteed for results. In order to prevent the singularity and limitation of a single

classifier, six CNNs are used for training. Then, the best four neural networks are ensembled based on the weighted voting method. Through multiple experiments, we find that when the accuracy is used as the weight, the classification result is the best.

(3). Excellent classification accuracy is achieved. The classification system can effectively overcome the problem of small datasets, while significantly reducing training time. On this basis, a classification accuracy of 98.90% is obtained.

This paper is divided into the following chapters: Section 2 introduces the related technologies of breast histopathological image classification. Section 3 discusses the proposed image classification method based on transfer learning and ensemble learning in detail. Section 4 introduces the experimental settings, process, analysis and limitation of the results. Section 5 summarizes this paper and puts forward the future plan under this topic.

2. Method

2.1. Related work

This part mainly introduces the related works involved in the paper and the research status in recent years.

2.1.1. Breast cancer and the application of CAD in breast histopathology

Among women, breast cancer accounts for one-quarter of cancer cases and one-sixth of cancer deaths. It ranks first in most countries (159 out of 185 countries) in morbidity and first in mortality among 110 countries [13]. In fact, women in all regions of the world are at risk of breast cancer at any age after puberty, and the incidence will increase in their later years.

The onset of breast cancer is caused by negative mutations in certain genes, after which breast tissue cancer is evolved into malignant tumors. There are two major types of breast cancer in medicine: carcinoma *in situ* and invasive carcinoma. Carcinoma *in situ* refers to the early stage of breast cancer where the growth of cancer cells is confined to ducts or lobules. Usually, the symptoms do not manifest themselves, and the possibility of spreading or metastasis is small. Over time, these cancer cells *in situ* may gradually develop and invade the surrounding breast tissue and then spread to nearby lymph nodes (specific regional metastasis) or other organs in the body (distant metastasis). This is called invasive carcinoma.

There are many pathogenic factors of breast cancer, mostly related to gender and age. Other reasons mainly include obesity [14], lack of healthy exercise [15], a high-protein diet, such as eating red meat with exogenous hormones or carcinogenic by-products [16], alcoholism [17], smoking [18], and using oral contraceptives [19]. These risk factors can be intervened through health education in clinical practice and public health programs. Unfortunately, even if all potential variables can be controlled, the risk of breast cancer can only be reduced by up to 30%.

Numerous significant advances in computer science and medicine have created exciting opportunities for medical experts and intelligent systems. CAD is the most direct and obvious result of the organic integration of the two. CAD does not rely on the analysis and skills of individual healthcare professionals and can make more objective and faster diagnostic decisions. In addition, CAD can narrow the gap between experienced and inexperienced medical personnel in diagnosis.

2.1.2. Deep learning model

Since 2012, the application of deep neural network (DNN) technology has become more and more extensive, including image preprocessing, feature extraction, image postprocessing, and classifier design. This development trend can be attributed to the rapid improvement of hardware performance, which provides high feasibility for realizing DNN algorithms with high computational complexity. In addition, an automatic feature extraction method can be realized by DNN, through which it can be more robust to extract complex microscopic breast tissue morphological features and structures. In the era of DNN, CNN is often preferred in image classification. Because of its superior performance in related fields, such as face recognition [20], autonomous driving [21], COVID-19 image analysis [22] and so on, CNN is also increasingly preferred in BHIC.

CNN is first proposed in [23], in which the backpropagation algorithm to the training of neural network structure is applied. Compared with traditional image classification methods, CNN-based deep learning can automatically learn features from massive amounts of data. Moreover, this method effectively reduces the interference of subjective

factors in the traditional method. At the same time, CNN has been well applied in many fields, including object or human body recognition, target tracking and detection, image segmentation and classification, natural language processing, etc. It has laid a good foundation for the application of CNN in BHIC.

VGGNet [24] is one of the top two networks in the ImageNet Large-Scale Visual Recognition Challenge (ILSVRC) [25] in 2014. The VGG16 and VGG19 models are simple in structure, but consume many resources, training time, and storage capacity. The Inception module is the core component of GoogLeNet [26]. Based on the first two versions, InceptionV3 uses the idea of factorization to split a two-dimensional convolution into two smaller modules: $n \times n$ convolution into $1 \times n$ and $n \times 1$ convolution. It is beneficial to reduce the number of parameters, speed up the calculation and further increase the depth and nonlinearity of the network. The Xception network is an improved version of InceptionV3 and is also regarded as an “extreme” version of the Inception [27]. The network introduces a deep separable convolution model, and an excellent effect can be obtained after comprehensive training data. One of the basic modules that make up ResNet [28] is called the residual block, which can effectively solve the problem of gradient disappearance in deep networks. DenseNet [29] is well-known for its particular structure. In forward propagation, each layer is directly connected with all previous layers, and the input of each layer comes from the output of all previous layers. Compared with the deep residual network, the number of parameters that need to be trained is much lower than that of ResNet to achieve the same accuracy.

With the proliferation of deep learning, people are increasingly pursuing stable models with good performance in all aspects, but the actual results are not so ideal. Therefore, the ensemble approach emerges as The Times require, which can complement every single classifier well. The work of [30] summarizes the recent applications in bioinformatics based on ensemble deep learning. Paper [31] further discusses the development and limitations of ensemble learning in the era of deep learning, which is instructive for our research.

2.1.3. *The development of breast histopathological image analysis*

In the past ten years, CNN has had an outstanding performance in BHIC. In [32], a third-party software (LNKNet package) containing a neural network classifier is applied to evaluate two specific textures, namely the quantity density of the two landmark substances, and a 90% classification accuracy of breast histopathology images is achieved.

In the paper [33], to classify breast histopathological images stained by H&E into four types, eight features and a three-layer forward/backward artificial neural network (ANN) classifier are applied. Finally, a classification accuracy of about 95% is obtained.

In [34, 35, 36], an automatic classification scheme is given. “Random subspace ensemble” is used to select and aggregate the designed classifiers. Moreover, a classification accuracy of 95.22% is obtained on a public image dataset.

In the paper [37], morphological features are extracted to classify cancer cells and lung cancer cells in histopathological images. In the experiment, the multi-layer perceptron based on the feedforward ANN model obtains 80% accuracy, 82.9% sensitivity, and 89.2% AUC successfully.

In [38], a CNN-based classifier of full-slice histopathological images is designed. First, the posterior estimate is obtained, which is derived from the CNN with specific magnification. Then, the posterior estimates of these random multi-views are vote-filtered to provide a slice-level diagnosis. Finally, 5-fold cross-validation at the patient-level is used in the experiment, with an average accuracy of 94.67%, a sensitivity of 96%, a specificity of 92%, and an F1-score of 96.24%.

In the paper [39], a ResHist model is designed to classify benign and malignant breast histopathological images, which is based on a 152-layer CNN with residual learning. In the experiment, the histopathology images are first enhanced, and then the ResHist model is trained end-to-end in the enhanced dataset by supervised learning. After testing by the ResHist model, the best accuracy of 92.52% and the F1-score of 93.45% are achieved. In addition, to study the recognition ability of the ResHist model for in-depth features, researchers input the extracted feature vectors into KNN, Random Forest [40], secondary discriminant analysis, and SVM classifiers. The best accuracy of 92.46% can be obtained when the deep functions are fed back to the SVM classifier.

In [41], a new hybrid convolutional and cyclic DNN is created to classify breast cancer histopathological images. The paper uses fine-tuned InceptionV3 to extract features for each image block. Then, the feature vectors are input to the 4-layer bidirectional long and short-term memory network [42] for feature fusion. In the experiment, the image is completely classified, and the average accuracy is 91.3%. It is worth noting that in this paper, a new dataset

containing 3,771 histopathological images of breast cancer is published, which covers as many different sub-categories of different ages as possible.

In [43], the deep CNN model based on the Haar wavelet is introduced to classify breast tissue pathological images, greatly reducing the calculation time and improving the classification accuracy. In the experiment, the accuracy of 98.2% and 96.85% are achieved for the BACH dataset of four and two types and the BreaKHis dataset of multiple types, respectively.

In the classification work of [44], an analysis technique based on deep learning is proposed. The technique first uses a method based on CNN and k -means for screening. Then ResNet50 is used to extract features, and P-norm pooling is used to get the final image features. In the end, SVM is applied for the final image classification, with an accuracy of 95%.

In [45], to distinguish four types of breast cancer in histopathological images, a novel deep learning method is introduced. In the method, hierarchical loss and global pooling are applied. VGG16 and VGG19 models are used as the base deep learning network, and a dataset containing 400 images is used for testing. Finally, an average accuracy of around 92% is obtained.

At present, there are a few types of research on the classification of breast histopathological images using ensemble learning methods. Among them, the classification based on patient-level labels is commonly studied, such as research in Table. 1.

Table 1. Research on the patient-level classification of breast histopathological images.

Year	Method	Dataset	Transfer Learning CNNs	Accuracy
2019	Ensemble of DNNs [46]	BreaKHis	VGG-19, MobileNet-V2, DenseNet-201	98.13%
2019	EMS-Net [47]	BreaKHis(40 ×)	ResNet-101, ResNet-152, DenseNet-161	99.75%
2020	Ensemble of DNNs [48]	Collected 544 Images	VGG-16, VGG-19	95.29%
2021	MCUa [49]	BreaKHis(40 ×)	ResNet-152, DenseNet-161	100.00%
2021	3E-Net [50]	BreaKHis(40 ×)	DenseNet-161, 6 image-wise CNNs	99.95%

From Table. 1, it can be seen that the existing methods have achieved outstanding results in patient-level classification tasks. Although patient-level classification is the most common clinical requirement, many studies classify breast histopathological images at the image level [51]. These tasks are generally combined with patient-level classification to train and test the proposed model, such as [52, 53, 54]. Nevertheless, since the image-level classification is more complex than the patient-level, the classification accuracy is not relatively high in previous research. Therefore, this paper focuses on the challenge of image-level classification. At the same time, the characteristics of each transfer learning model are comprehensively considered, and ensemble learning is carried out based on their complementarity.

2.2. Our method

2.2.1. Transfer learning

Transfer learning is a method of applying knowledge or patterns learned in a specific field or task to different fields or problems [55]. Traditionally, machine learning algorithms have strict training and test data requirements, which require them to obey the same distribution. However, in reality, this hypothesis cannot be fully established, resulting in many restrictions on the practical application of machine learning. At the same time, the acquisition of sufficient training data is another big problem for researchers. Therefore, scholars have developed a special method to use a large amount of easy-collected data from different fields to train learners and apply them to other similar scenarios. This method is called transfer learning. In other words, if X_S stands for the feature space and X_T stands for the label space, given a source domain $D_S = \{X_S, f_S(x)\}$ and learning task T_S , a target domain $D_T = \{X_T, f_T(x)\}$ and learning task T_T , transfer learning aims to help improve the learning of the target predictive function $f_T(x)$ in D_T using the knowledge in D_S and T_S , where $D_S \neq D_T$, or $T_S \neq T_T$. As for neural networks, researchers can directly use pre-trained models through a large number of ready-made datasets. Then, reusable layers are selected, and the output of these layers is used as input to train a network with fewer parameters and a smaller scale. This small-scale network only needs to clarify the internal relationships of specific problems and learn the implicit patterns through pre-trained models [56].

At present, there are two main methods of applying transfer learning: one is to fine-tune the parameters of the pre-trained network according to the required task; the other is to use the pre-trained network as a feature extractor and then use these features to train a new classifier. In this paper, we choose the former one.

The reasons why transfer learning is selected in this paper are as follows:

(1). Well-labeled histopathological images of breast cancer are relatively limited. Due to the complexity of such images, it is costly for medical experts to annotate data. Therefore, few publicly large-scale image datasets are available. Fortunately, transfer learning can effectively overcome the problem of insufficient data [57].

(2). In the classification task of histopathology images, most of the preprocessing models come from ILSVRC. Because of their stability in specific challenges, they can be safely applied in breast cancer classification tasks.

(3). Transfer learning helps to improve accuracy or reduce the training time [58], which is a crucial reason why transfer learning is widely welcomed.

In this paper, the VGG series, Inception series, ResNet series, and DenseNet series are carefully studied and compared, and six CNNs are selected to classify breast histopathological images into benign and malignant tumors. They are: VGG16, VGG19, InceptionV3, Xception, ResNet50 and DenseNet201. These classic networks are selected because, on the one hand, these networks have passed numerous classification tasks and have shown high accuracy and stability in various datasets. In addition, the advantages and shortcomings of these networks are systematically considered, and it is highly possible to build a comprehensive ensemble network by using their complementarity.

For VGGNet, the VGG16 and the VGG19 network model are selected, because of their simple network structure and excellent learning performance on many tasks. In terms of the classification ability and parameter quantity, InceptionV3 and Xception network models are adopted for the Inception series. In the ResNet series and the DenseNet series, considering the calculation ability and other issues, we finally choose the ResNet50 and the DenseNet201 network model to conduct the research. In summary, six CNN models of VGG16, VGG19, InceptionV3, Xception, ResNet50, and DenseNet201 are applied to the classification of breast histopathology images.

In the transfer learning based on these six CNNs, first of all, the massive labeled images in the ImageNet dataset are applied separately, so these networks have good classification capabilities. Then, the front ends of the trained model parameters in these six CNNs are all frozen, so as not to destroy any information they contain in future training. After that, the augmented breast histopathological images and their labels are used to fine-tune the fully connected layers at the back end of the six networks. Finally, the classification ability learned on ImageNet can be transferred to the given pathological slices.

2.2.2. Ensemble learning

In the past few decades, ensemble learning has received more and more attention in the field of computational intelligence and machine learning. Ensemble learning is a process in which multiple models, such as classifiers, are combined according to a certain method to solve a specific intelligent computing problem. It is mainly used to improve the performance of the final model, such as classification, prediction, and function estimation, or to reduce the impact of improper selection of the basic model.

The general framework of ensemble learning is summarized as follows: First, a group of individual learners is generated; after that, the learners are effectively combined through a specific strategy; finally, the expected experimental results can be obtained [59]. Individual learners are usually generated from training data by existing learning algorithms (such as decision tree and error propagation neural network). Among them, using individual learners of the identical type (such as all neural networks) is called homogeneous ensemble learning, and applying various individual learners is called heterogeneous ensemble learning. In this paper, homogeneous ensemble learning is used.

Recent fast ensemble deep learning techniques [60, 61] can be applied in whole slide medical image analysis (f.e. predicting pCR from H&E stained whole slide images [62]) to reduce time and space overheads at the expense of certain accuracy. However, we believe that performance improvement is more critical in this task, so we choose some usual ensemble methods. There are three general combination strategies: voting, averaging, and stacking. Nevertheless, for the task of this paper that aims to achieve the binary classification of breast histopathological images, the voting method is the most commonly used and easily manipulated one. This method refers to the assumption that there are T different classifiers h_1, h_2, \dots, h_T , and our goal is to predict the final category from the l category markers c_1, c_2, \dots, c_l based on the output of the classifier. Typically, for the sample x , the output result of the classifier h_i is an l -dimensional label vector $(h_i^1(x), h_i^2(x), \dots, h_i^l(x))^T$, where $h_i^j(x)$ is the prediction output of the h_i classifier on the class c_j label.

Voting can be divided into three types. Absolute majority voting: Different categories will be marked by each classifier for voting. If the final number of votes obtained by a certain type of mark exceeds $\frac{1}{2}$, the category is regarded as the final output result; if the votes for all the categories do not exceed $\frac{1}{2}$, the forecast is rejected. Relative majority voting: The side with the most votes is deemed the winner; when there is a tie, one side is chosen arbitrarily. Weighted voting: Different from the previous two, the corresponding weights are assigned to different classifiers; if the classifier performs better, a higher weight is assigned. Finally, the weighted votes of each category are summed, and the one corresponding to the maximum value is regarded as the final result.

Although there are endless ensemble learning methods, considering their complexity and ease of operation, the basic weighted voting strategy is applied in this paper, and the formula is Eq. (1). When given appropriate weights, weighted voting can be both superior to the individual classifier with the best classification result, and at the same time, superior to the absolute majority voting.

$$H(x) = c_{arg,max} \sum_{i=1}^T w_i h_i^j(x) \quad (1)$$

Among them, w_i represents the weight of the classifier h_i . In practical applications, similar to the weighted average method, the weight coefficients are often normalized and are constrained to be $w_i \geq 0$ and $\sum_{i=1}^T w_i = 1$. Getting the right weight is very important. Suppose $l = (l_1, l_2, \dots, l_T)^T$ is the output of the individual classifier, where l_i represents the prediction result of the class label of the classifier h_i on sample x . Let p_i be the precision of h_i , the combined output of the category label c_j can be expressed as Eq. (2) using a Bayesian optimal discriminant function.

$$H^j(x) = \log(P(c_j)P(l|c_j)) \quad (2)$$

When it is assumed that the output conditions of individual classifiers are independent, Eq. (2) can be reduced to Eq. (3).

$$H^j(x) = \log P(c_j) + \sum_{i=1}^T h_i^j(x) \log \frac{p_i}{1 - p_i} \quad (3)$$

When the first term of the above equation does not depend on the individual classifier, the optimal weight of the weighted voting can be obtained from the second term and satisfies Eq. (4).

$$w_i \propto \log \frac{p_i}{1 - p_i} \quad (4)$$

Therefore, the optimal weight needs to be consistent with the performance of the individual classifier, which is based on the case where the output of the individual classifier is independent of each other. However, in the actual work of this paper, the classifier is trained for the same problem. The output is usually strongly correlated, and the independence assumption is not valid. So the weight is set based on the evaluation indicators of the classifier, which is also a commonly used method of weighting.

3. Result

3.1. Experimental settings

3.1.1. Image dataset

To implement the proposed model, a practical open-source BreaKHis dataset is used in the research of this paper [63]. BreaKHis consists of 7,909 clinically representative microscopic images of breast tumor tissue, which are collected from 82 patients using four magnifications.

Data source: The sample comes from a biopsy section of breast tissue, which is marked by pathologists in Brazil's P&D laboratory;

Staining method: H&E staining;

Magnification: 50×, 100×, 200×, 400×;

Microscope: Olympus BX-50 system microscope, with 3.3 times magnification relay lens, connected with Samsung digital color camera SCC-131AN;

Camera pixel size: $6.5 \mu\text{m}$;

Image size: 700×460 pixels;

Image format: *.png;

Pixel bit depth: 24 bits (RGB three-channel image, 8 bits per channel, $3 \times 8 = 24$);

Up to now, a total of 2,480 benign tumor samples and 5,429 malignant tumor samples have been collected in the BreakHis dataset. Both of them are divided into different subtypes, respectively. As shown in Fig. 3, the first line is the four subtypes of benign tumors, including Adenosis (A), Fibroadenoma (F), Tubular Adenoma (TA), and Phyllodes Tumor (PT). The second line is the four subtypes of malignant tumors, including Ductal Carcinoma (DC), Lobular Carcinoma (LC), Mucinous Carcinoma (MC), and Papillary Carcinoma (PC).

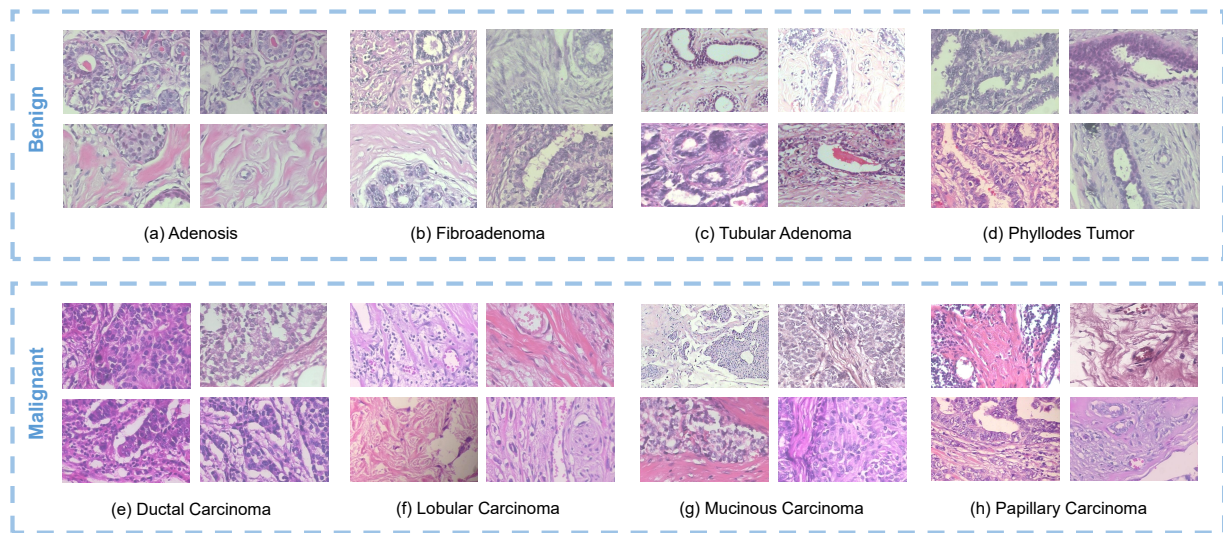


Figure 3. Benign/malignant tumor subtype samples

Therefore, the dataset can be used for both binary classification and multi-classification tasks. In this paper, the binary classification of benign/malignant tumors under four magnifications is studied. Table 2 shows the distribution of samples in this dataset.

Table 2. Image distribution by magnification factor and class.

Magnification	Benign	Malignant	Total
40×	625	1,370	1,995
100×	644	1,437	2,081
200×	623	1,390	2,013
400×	588	1,232	1,820
Total	2,480	5,429	7,909
Number of patients	24	58	82

3.1.2. Setting of experimental data

In clinical work, patient-level classification is essential. In the early pre-experiment and review [12], it has been found that many methods can achieve excellent classification results under the label of the patient. However, because the data information under the same patient label is highly correlated, the patient-level classification is not challenging enough. Therefore, the lower-level classification based on the image label is applied, and a better result is achieved in the preliminary experiment.

This experiment uses a cross-validation method to separate the BreKHis dataset into three mutually exclusive subsets. The subsets are randomly selected from the dataset at a ratio of 7:1:2 and are separated into the training set, validation set and test set. However, according to the introduction of the dataset above, it is evident that the number of images under the two categories of benign (2,480) and malignant (5,429) is seriously imbalanced. Approximately 69% of images are samples of malignant tumors. In order to tackle this problem, data augmentation strategies are applied to the benign tumor samples in all of the subsets, namely horizontal mirror flip and vertical mirror flip, with a total of 2,480 images generated. Afterward, 469 images are randomly selected from the data obtained through the vertical mirror flip through calculation. Finally, based on the original data volume (2,480), adding the horizontal mirror flip (2,480) and the selected vertical mirror flip dataset (469), the benign sample reaches 5,429 images. In this way, the number of images in both two categories is equal, with 10,858 images. The amount of samples in each subset is presented in Table 3. In the early research [64], we did data augmentation based on Generative Adversarial Network (GAN) and achieved relatively good results. However, the focus of this paper is not to generate a large number of new datasets, and only using mirror flipping can satisfy this experiment.

Table 3. Data setting.

	Benign	Malignant	Total
Training set	3,800	3,800	7,600
Validation set	543	543	1,086
Test set	1,086	1,086	2,172

3.1.3. Experimental environment

The experiments involved in this paper are all developed based on the Python language (version 3.6.8) under the Windows 10 operating system. All deep learning models involved in the experiment are developed (training, test) entirely by the Keras (version 2.24) framework. In addition, TensorFlow (version 1.12.0) is used as the backend of Keras. The specific conditions of the workstation parameters applied in the experiment are as follows: Intel(R) Core(TM) i7-8700 CPU (3.20 GHz), 32GB RAM, NVIDIA GEFORCE RTX 2080 8 GB.

3.2. Evaluation metrics

In the course of our experiments, the performance of the classifier needs to be quantitatively evaluated. Appropriate evaluation indicators can reduce the deviation of algorithm differentiation. In this paper, confusion matrixes are used to analyze various evaluation measures. For the n -type classification problem, the confusion matrix is a table of size $n \times n$. An accurate classifier represents most samples along the diagonal of the matrix. In fact, the confusion matrix itself is not a performance indicator, but almost all frequently-used indicators are based on it. Table 4 is a confusion matrix based on two classifications. Positive samples can be regarded as samples of research interest. Thus, we consider samples of benign tumors as positive and samples of malignant tumors as negative.

Table 4. Confusion matrix based on binary classification.

Output class	Target class	
	Positive (P)	Negative (N)
Positive (P)	TP	FP
Negative (N)	FN	TN

TP (True Positive) is that an example is correctly identified as a positive; TN (True Negative) is that an example is correctly identified as a negative; FP (False Positive) is that negative cases are misclassified as positive ones; FN (False negative) is that positive instances are incorrectly classified as negative. This experiment evaluates the performance of six CNN classifiers mentioned above based on these four values.

For classification tasks, accuracy, precision, recall and F1-score are considered the most popular techniques for measuring the classification results. These evaluation indicators are described in Table 5. The accuracy is the ratio

Table 5. Evaluation metrics.

Assessment	Formula
Accuracy	$\frac{TP+TN}{TP+FP+FN+TN}$
Precision	$\frac{TP}{TP+FP}$
Recall	$\frac{TP}{TP+FN}$
F1-score	$\frac{2 \times P \times R}{P+R}$

of the number of correctly classified samples to the total number of samples. The precision reflects the proportion of true positive cases in the cases that are judged to be positive, which represents how many benign tumors are predicted to be correct. The recall reflects the proportion of cases judged to be positive in the total number of positive cases. Low recall means that many patients with benign tumors are treated as cancer, which is a major medical incident. Therefore, recall is of great significance in medical image diagnosis. However, precision and recall are contradictory to a certain extent. If the precision is intended to be improved, it can be achieved by raising the criteria for positive classification. In other words, the number of samples predicted to be positive is reduced. Although the precision has improved, the recall will definitely decrease. On the contrary, if the recall needs to be improved, all samples can be marked as positive. In this way, the recall can reach 100%, but the precision will be absolutely reduced. Therefore, $F\beta$ -score is introduced, which is a vital technique that balances precision and recall. When $\beta = 1$, it is the harmonic average of the two values, namely the F1-score.

3.3. Deep learning algorithm

3.3.1. CNN training process

The training process of CNN is divided into two stages: forward propagation and back propagation. The flow chart of its training is shown in Fig. 4. The whole training process includes (a) Forward Propagation and (b) Back Propagation. In forward propagation, six network models VGG16, VGG19, InceptionV3, Xception, ResNet50 and DenseNet201 are loaded first, and the weights of these neural networks are initialized. After that, the training data is input, and the output results are obtained through the convolutional layer, the lower sampling layer and the full connection layer. Next, the error between output and target value is calculated. When the error meets the requirements, the weights and thresholds of each layer are saved. If not, the process of back propagation is entered, which intends to update the weight to reduce error. If the performance does not improve, the learning rate will be decayed. Then return to start the next iteration. The process for each CNN is summarized in Algorithm 1.

Apart from transfer learning, six CNNs are also trained from scratch as a comparative experiment. Table 6 summarizes the parameters of these models. Among them, both Top-1 Accuracy and Top-5 Accuracy refer to the accuracy of each neural network on the ImageNet validation set. Depth refers to the topological depth of each neural network, including the activation layer and batch normalization layer.

3.3.2. Classification performance evaluation

In the classification of breast histopathological images, some hyperparameters are set. After many trials, these values are taken when the validation set obtains the best result. The exponential decayed learning rate is adopted regardless of training from scratch or training based on transfer learning. The decay steps are set to 5, the decay rate is 0.1, the initial learning rate is 1×10^{-4} , and the adaptive moment estimation (Adam) is selected as the optimizer. The other hyperparameter settings in the experiment are as follows:

Training the network from scratch: The initial input size is $224 \times 224 \times 3$, and the batch sizes of the VGG16, VGG19, InceptionV3, Xception, ResNet50, and DenseNet201 networks are set to 32, 16, 26, 8, 26 and 16, respectively. The epoch is specified as 60.

Transfer learning network: The initial input size is $460 \times 460 \times 3$, the batch size is set to 16, and the epoch is 60. In Table 7, the classification results obtained by the above six CNNs based on these two training methods are summarized respectively.

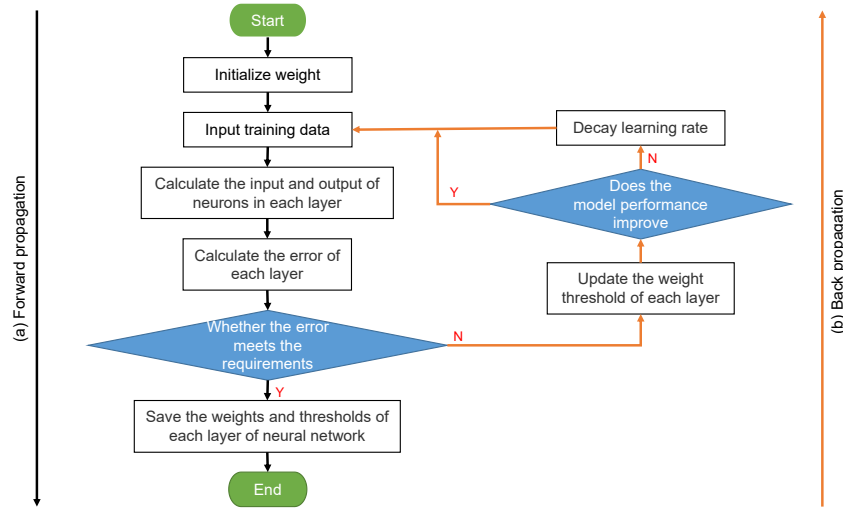


Figure 4. The workflow of neural networks.

Algorithm 1: Transfer learning algorithm in this paper

Input: The labeled dataset S , a base learning **Classifier** pre-trained on ImageNet, and the maximum number of iterations N .

- 1 **Initialize** the initial weight vector, that w_{jk}^l is the weight from the k^{th} neuron in the $(l-1)^{\text{th}}$ layer to the j^{th} neuron in the l^{th} layer. b_j^l and a_j^l are the bias and the the activation (the output of the activation function) of the j^{th} neuron in the l^{th} layer, respectively.
- 2 **while** this model is improved **do**
- 3 **if** not first time executing this code **then**
- 4 Attenuating the learning rate
- 5 **for** $t = 1, \dots, N$ **do**
- 6 Suppose the input is X and the output is Y . The value of a_j^l depends on the activation of the previous layer of neurons: $a_j^l = \sigma(\sum_k w_{jk}^l a_k^{l-1} + b_j^l)$;
- 7 Rewrite the formular above into a matrix form: $a^l = \sigma(w^l a^{l-1} + b^l)$;
- 8 Call **Classifier**, calculate the activation using $a^l = \sigma(w^l a^{l-1} + b^l)$ layer by layer, $X \rightarrow \hat{Y}$;
- 9 Calculate the loss function: $C = \frac{1}{2n} \sum_x \|y(x) - a^L(x)\|^2$. Where n is the total number of training samples x , $y = y(x)$ is the ground truth, L is the number of layers of the network, and $a^L(x)$ is the output vector of the network;
- 10 Calculate the value of w when the error is the smallest by taking the partial d erivative of w_{jk}^l ;
- 11 **Update** the weights in the direction of reducing errors;

Output: the CNN with trained weights and thresholds for each layer.

From the statistical table of classification results, it can be concluded that the effect of transfer learning is generally better than that of training from scratch. Through transfer learning, the accuracy can be increased by around 3% to 14%, which is a very satisfactory result. In addition, it is also found that training the InceptionV3 network from scratch is better than any other network using this method for training. At the same time, the accuracy of InceptionV3 training from scratch is 0.65% higher than that of transfer learning. Both the recall and the F1-score are also higher than using transfer learning, with the values of 99.26% and 94.73%, respectively. Nevertheless, this does not affect our subsequent choice of InceptionV3 based on transfer learning for the next step. This is because the training time of the network from scratch is generally more extended, and the performance of the computer should also be taken into

Table 6. Overview of CNN parameters.

Model	Size	Top-1 Accuracy	Top-5 Accuracy	Parameters	Depth
VGG16	528 MB	71.3%	90.1%	138,357,544	23
VGG19	549 MB	71.3%	90.0%	143,667,240	26
InceptionV3	92 MB	77.9%	93.7%	23,851,784	159
Xception	88 MB	79.0%	94.5%	22,910,480	126
ResNet50	98 MB	74.9%	92.1%	25,636,712	—
DenseNet201	80 MB	77.3%	93.6%	20,242,984	201

Table 7. The result and prediction time of CNN models on validation set (unit, %).

Model	Training Mode	Accuracy	Precision	Recall	F1-score	Time (unit, s)
VGG16	Training from scratch	89.50	89.65	89.32	89.48	17.28
	Transfer Learning	95.49	95.40	95.58	95.49	32.50
VGG19	Training from scratch	91.34	90.16	92.82	91.47	17.96
	Transfer Learning	95.03	93.27	97.05	95.13	38.61
InceptionV3	Training from scratch	94.48	90.59	99.26	94.73	42.75
	Transfer Learning	93.83	97.41	90.06	93.59	52.99
Xception	Training from scratch	89.96	86.29	95.03	90.45	31.04
	Transfer Learning	96.59	94.54	98.90	96.67	39.45
ResNet50	Training from scratch	84.71	94.15	74.03	82.89	34.97
	Transfer Learning	98.90	98.72	99.08	98.90	42.72
DenseNet201	Training from scratch	88.03	95.19	80.11	87.00	94.14
	Transfer Learning	98.25	96.95	99.63	98.27	103.06

account. In the same environment, training each network from scratch usually takes more than 2 hours. Therefore, transfer learning is applied to all the networks for the following research.

3.3.3. Overall evaluation and visual analysis transfer learning networks

Fig. 5 shows the transfer learning training curves of the six CNNs: VGG16, VGG19, InceptionV3, Xception, ResNet50 and DenseNet201, respectively, to observe the changes in the training process of these models. It includes training set accuracy curve (blue curve), training set loss curve (green curve), validation set accuracy curve (yellow curve), validation set loss curve (red curve). As the number of training rounds increases, the accuracy curve shows an upward trend, and the loss curve shows downward. This is what we expected, which means that the performance of the models is gradually becoming stable.

Subsequently, these six networks are compared, and their confusion matrices are shown in Fig. 6.

In the end, the ResNet50 network performs best, with three indicators that top all network models. To be precise, the accuracy is 98.90%, the precision reaches 98.72%, and the F1-score reaches 98.90%. The second place is the DenseNet201 network, which is comparable to the ResNet50 network, at around 98%. Moreover, the recall of the DenseNet201 network is the highest among all models, reaching 98.63%. In order to analyze the classification results more intuitively, their evaluation indicators are drawn into a histogram, as shown in Fig. 7. In addition, we integrate the metrics and further calculate the average precision (AP) to evaluate the overall results. AP originates from the field of information retrieval and is primarily used to evaluate ranked lists of retrieved samples. The definition of AP in the experiment is shown in the Eq. 5:

$$AP = \frac{\sum_{n=1}^{i=1} (P(t)) \times rel(t)}{N} \quad (5)$$

N is the number of relevant histopathology images, $P(t)$ is the t -th position in the list divided by considering the cutoff position, and $rel(t)$ is an index. The image ranking of the t -th position is the target type image, then it takes 1;

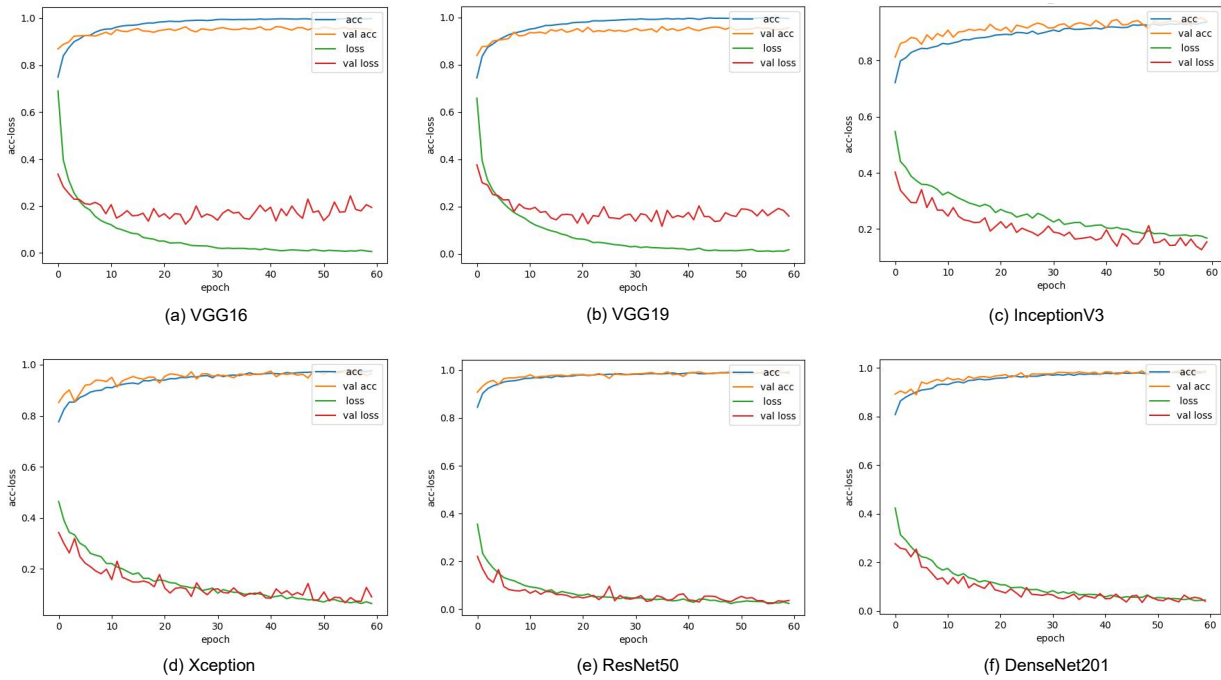


Figure 5. CNN training process curve.

otherwise, it takes 0. AP represents the average value of the image accuracy of the target type at the current location. Furthermore, we apply mean AP (mAP) to summarize the AP for each class. It is calculated by taking the average value of AP as shown in the table 8. Except for InceptionV3, the other five networks all perform well, all of which are above 80% in mAP.

Table 8. The AP and mAP of each model on validation set (unit, %).

Model	AP (malignant)	AP (benign)	mAP
VGG16	83.79	79.30	81.55
VGG19	86.52	84.54	85.53
InceptionV3	70.56	71.10	70.83
Xception	84.40	85.40	84.90
ResNet50	85.00	84.47	84.73
DenseNet201	83.27	86.10	84.68

In the final evaluation, the results of the InceptionV3 network are relatively the worst, in which the accuracy, recall, F1-score and mAP are the lowest among the six models, with 94.48%, 90.06%, 93.59% and 70.80%, respectively. The lowest precision is obtained on VGG19, which is 93.27%. For networks that belong to the same series, such as the VGGNet series, the overall performance of the VGG16 network is better than that of the VGG19 network. Three indicators calculated in the VGG16 network are about 0.3% to 2% higher than those in the VGG19 network. For the Inception series, the performance of the Xception network is better than that of the InceptionV3 network, and three of the evaluation indicators are about 2% to 8% higher than the InceptionV3. The performance of the DenseNet201 network and the ResNet50 network are relatively good, with satisfactory classification results. Finally, referring to the size, parameter amount, and network depth of the CNNs in Table 6, four networks are chosen in the end, namely VGG16, Xception, ResNet50 and DenseNet201 for the follow-up ensemble experiment.



Figure 6. Confusion matrix of CNN on validation set.

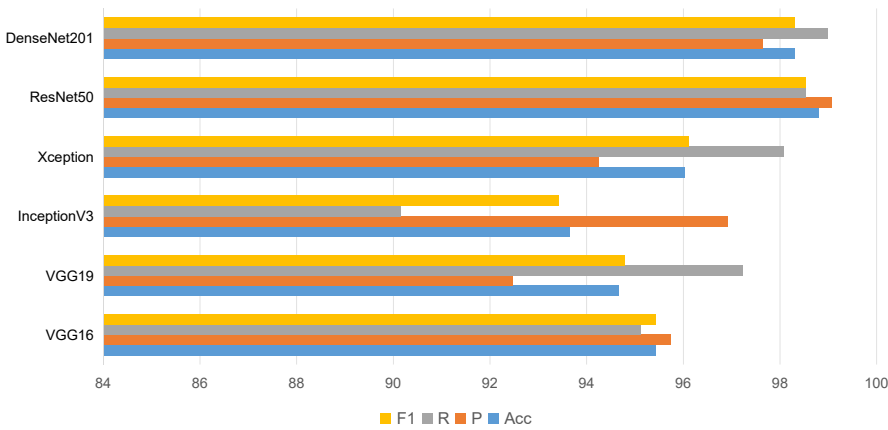


Figure 7. Comparison of evaluation indicators among six CNNs (unit, %). The horizontal axis shows the value of the evaluation index, the vertical axis represents six different models, and the rectangular bars of different colors represent four evaluation indicators.

3.4. Ensemble learning

3.4.1. Ensemble pruning

Ensemble pruning refers to selecting a subset of the individual learners that have been trained instead of all learners for the next step. It has two advantages: First, the ensemble result can be obtained using a smaller network scale. This can not only reduce the storage overhead brought by storing model, but also reduce the computing overhead

corresponding to the output of the individual learner, thereby improving the efficiency of the model. In addition, the generalization performance of ensemble pruning is even better than the ensemble obtained by using all individual learners.

In this paper, two classifiers with relatively poor performance are pruned from the six CNN models based on transfer learning, and four classifiers are selected as individual learners, namely VGG16, Xception, ResNet50, and DenseNet201 models. Since the accuracy is the main evaluation index of this experiment, the *Accuracy* of each network is used as the weight of our voting method. Firstly, each weight is quantized with the step length 0.01 into {0, 0.01, 0.02, ..., 0.99, 1}. Then, in a weigh vector $w_{k=1,2,\dots,6}$, the combination of $w_{(k,1)}$, $w_{(k,2)}$, $w_{(k,3)}$ leads to the highest matching accuracy $Accuracy_k$ is chosen. Finally, the selected $w_{k=1,2,\dots,6}$ are implemented the ensemble learning method. And finally, we got the best ensemble accuracy of 98.90% in this way.

Thus, the final experimental procedure is obtained. First, in order to achieve data balance, data augmentation is applied to the BreaKHis dataset. The method used in this procedure is horizontal and vertical mirror flip. Then, the augmented data is input into each transfer learning based CNN, and six individual classifiers are obtained. After that, four classifiers with relatively good performance are selected and trained using the ensemble learning strategy of weighted voting. Finally, the ensemble results are evaluated.

3.4.2. Evaluation of ensemble learning algorithms

After training, the four indicators of accuracy, precision, recall, and F1-score are still used to evaluate the overall performance of the system. Fig. 8 shows the confusion matrix of ensemble learning. It can be found that the algorithm based on ensemble learning predicts 1 sample that should be benign as malignant and predicts 11 samples that should be malignant as benign.

Confusion Matrix

Output class	benign	542 49.91%	11 1.01%	98.01% 1.99%
	malignant	1 0.09%	532 48.99%	99.81% 0.19%
		99.82% 0.18%	97.97% 2.03%	98.90% 1.10%
		benign	malignant	
		Target class		

Figure 8. Confusion matrix of ensemble learning on the validation set.

Finally, the overall indicators of all single CNNs and our ensemble method are evaluated on the test set and summarized in Table 9. The ensemble learning strategy finally achieves 98.90% accuracy, 98.72% precision, 99.08% recall, 98.90% F1-score and 98.63% mAP. Obviously, the accuracy, recall, F1-score and mAP are higher than using any of the six CNNs based on transfer learning alone. After comparison, this method effectively improves the accuracy by 0.1% to 5.25%, the recall by 0.09% to 8.93%, the F1-score by around 0.3% to 5%, and mAP by around 0.2% to 20%. In terms of precision, although it does not exceed the 99.07% achieved by the ResNet50 network, its performance surpasses the other five models and wins second place. In summary, the classification performance of the ensemble learning method is generally better than that of the single transfer learning method.

Table 9. Summary of classification results in testing process (unit, %).

Model	Evaluation metrics				
	Accuracy	Precision	Recall	F1-score	mAP
VGG16	95.44	95.74	95.12	95.43	96.45
VGG19	94.66	92.47	97.24	94.79	95.89
InceptionV3	93.65	96.93	90.15	93.42	77.12
Xception	96.04	94.25	98.07	96.12	96.88
ResNet50	98.80	99.07	98.53	98.53	95.57
DenseNet201	98.30	97.64	98.99	98.31	98.47
Ensemble	98.90	98.72	99.08	99.90	98.63

4. Discussion

4.1. Comparative experiment

To evaluate the ability of the breast histopathological image classification algorithm proposed in this paper, a comparative experiment on Transformer and MLP models is carried out using the dataset divided by this experiment. The latest methods are summarized in Table. 10, which have shown great power in natural image classification. However, their generalization ability has not been developed well like CNN for the specific histopathological images, and the overall classification performance is not so good. Especially Transformer, because of its good ability to describe global information, there should be improved versions suitable for pathological images in the near future, making novel contributions to this field.

Table 10. Comparison of accuracy between the existing method and our method on the same BreakHis dataset.

Model		Accuracy (unit, %)	Training time (unit, s)
Transformer	BoTNet-50 [65]	90.75	4502
	CaiT [66]	96.70	5081
	CoaT [67]	92.91	420
	DeiT [68]	90.51	2101
	LeViT [69]	93.42	13321
	ViT [70]	80.11	1242
	T2T-ViT [71]	80.02	2370
MLP	MLP-mixer [72]	83.84	5541
	gMLP [73]	93.88	8407
	ResMLP [74]	79.56	10341
Our method	Ensemble transfer learning model	98.90	3245

4.2. Comparison of previous research

As can be seen from Table. 9, although compared to some single classifiers, the accuracy of our ensemble network has not been significantly improved. However, the network has been enhanced in the evaluation of the four indicators. In particular, F1-score is even close to 100%, reflecting that both precision and recall of the model are excellent.

Fig. 9 shows the comparison of some images that are not correctly classified and those that are correctly classified. It can be found that the correctly classified image contains almost all classification information of benign and malignant so that the proposed algorithm can easily identify it. There are two main reasons why the image is mispredicted. First, this type of image has a very high degree of similarity to another type, such as Fig. 9 (a) and Fig. 9 (b). When one type of image is similar to another type of texture, distribution and color, it will not be easy to identify correctly. In addition, the wrongly predicted images often contain very little information to distinguish between benign and

malignant, such as Fig. 9 (c) and Fig. 9 (d). Patch-based images are allowed to contain many blanks during segmentation. The abovementioned reasons can interfere with the model's correct classification of benign and malignant breast histopathological images.

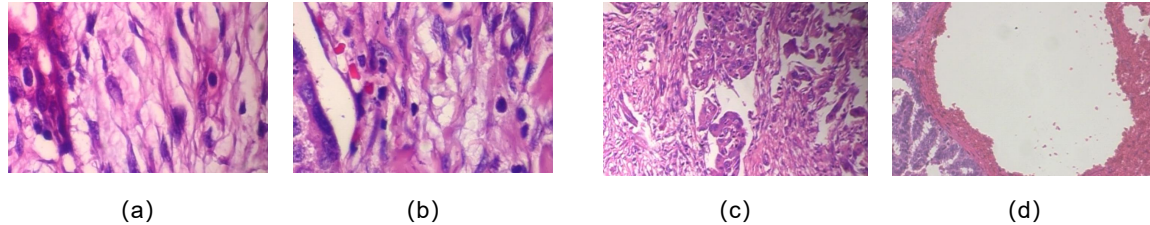


Figure 9. An example of the classification result. (a) and (c) are correctly classified images. (b) and (d) are wrongly classified images.

Additionally, we analyze the works based on deep learning on the BreakHis dataset. Especially for image-level classification in previous research, such as [53] with around 96% and [54] with 94%, our method with 98.90% accuracy works more effectively. Other ANNs and their results in different tasks are summarized in Table. 11, which are all applied in BreakHis dataset. It should be noted that some studies may have done both binary and multiple classifications, but only the former results are considered. When compiling the tables, it is found that only a few studies used evaluation indicators other than accuracy. Even if the same indicator is employed (specifically, precision, recall and F1-score), the proposed method in this paper has a better performance. To facilitate statistics, only the accuracy of each study is discussed in detail. From the table, it can be concluded that in these algorithms, the accuracy of our method is effectively improved by 0.13% to 21.4%.

5. Conclusion and future work

In this paper, a framework that combines transfer learning and ensemble learning is proposed for the image-level classification of breast histopathological images. Finally, an accuracy of 98.90% is obtained. First of all, based on the pre-segmented BreakHis dataset, training from scratch and transfer learning are applied separately to train the six selected neural networks. Meanwhile, confusion matrices are used for the comparison and analysis of algorithms. Considering the two perspectives of less training time and high accuracy, we select the transfer learning method. After that, based on the idea of ensemble pruning, four networks are selected as individual classifiers. Through a large number of experiments, the weighted voting method with accuracy as the weight is used to combine these classifiers. Finally, we use the ten latest Transformer and MLP models to classify breast histopathological images on the same image-level dataset. It turns out that our method is quite competitive and ranks first in accuracy.

This research is dedicated to developing an algorithm to assist doctors in diagnosing tumor types correctly. The goal is to promote the calculation speed and efficiency, as well as the reliability of the final classification results. However, there is still massive potential for further exploration and development. Firstly, classifiers with better performance can be selected to further improve the final classification effect. Secondly, in addition to the weighted voting method used in this paper, more ensemble strategies and weights can be discussed in more depth. In addition, there are many types of breast cancer and many subtypes of tumors. This work is a two-class classification at the image level. In the future, a multi-classification system can be introduced on this basis. Henceforth, we are committed to continuously developing more efficient and high-accuracy classification models and will get involved in the image-level multi-classification tasks.

Author Contributions

Yuchao Zheng: method, experiment, result analysis and paper writing. Chen Li: method, result analysis, paper writing and proofreading. Xiaomin Zhou: method, experiment. Haoyuan Chen: comparative experiment. Hao Xu, Xinyu Huang and Marcin: data analysis, proofreading. Yixin Li: comparative experiment. Haiqing Zhang: paper

Table 11. Comparison of accuracy between the existing methods and our method based on BreaKHis dataset (unit, %).

Year	Types of ANN that based on	Level	Overall accuracy
2016	CNN [75]	patient	83.25
2016	AlexNet [76]	patient	84.53
		image	84.40
2017	CaffeNet [77]	patient	84.15
		image	83.80
2017	CNN [78]	patient	88.03
		image	85.33
2017	CNN based on VGGNet [79]	patient	84.85
2017	CNN [80]	patient	77.50
2017	CSDCNN [81]	patient	93.20
2017	BiCNN [82]	patient	97.41
		image	97.77
2018	VGG16 [83]	patient	92.60
2018	RNN and CNN [84]	patient	91.00
2018	DCNN [85]	patient	92.19
2018	CNN [86]	image	90.00
2018	DenseNet based CNN [87]	patient	95.40
2018	ResNet [88]	patient	98.77
2018	DCNN [89]	patient	85.30
2019	SA-Net [90]	patient	96.00
2019	CNN [91]	patient	96.24
2019	DCNN [92]	patient	97.90
2019	VGG16 and VGG19 [93]	patient	98.10
2020	ResHist [39]	patient	88.98
		image	88.02
2020	DSoPN [53]	patient	96.51
		image	96.54
2021	myResNet-34 [54]	image	94.03
2022	Our method	image	98.90

writing. Xiaoyan Li and Hongzan Sun: medical knowledge. All authors contributed to the article and approved the submitted version.

Acknowledgements

This work is supported by National Natural Science Foundation of China (No. 61806047). We thank Miss Zixian Li and Mr. Guoxian Li for their important discussion.

Conflict of Interest

The authors declare that they have no conflict of interest in this paper.

References

- [1] [EB/OL]. 2020. <https://gco.iarc.fr/today/data/factsheets/cancers/20-Breast-fact-sheet.pdf>.
- [2] Murtaza G, Shuib L, Abdul Wahab A W, et al. Deep learning-based breast cancer classification through medical imaging modalities: state of the art and research challenges[J]. Artificial Intelligence Review, 2020, 53(3): 1655-1720.

- [3] Domingues I, Pereira G, Martins P, et al. Using deep learning techniques in medical imaging: a systematic review of applications on ct and pet[J]. *Artificial Intelligence Review*, 2020, 53(6): 4093-4160.
- [4] Kozegar E, Soryani M, Behnam H, et al. Computer aided detection in automated 3-d breast ultrasound images: a survey[J]. *Artificial Intelligence Review*, 2020, 53(3): 1919-1941.
- [5] Moghbel M, Ooi C Y, Ismail N, et al. A review of breast boundary and pectoral muscle segmentation methods in computer-aided detection/diagnosis of breast mammography[J]. *Artificial Intelligence Review*, 2020, 53(3): 1873-1918.
- [6] Moghbel M, Mashohor S. A review of computer assisted detection/diagnosis (cad) in breast thermography for breast cancer detection[J]. *Artificial Intelligence Review*, 2013, 39(4): 305-313.
- [7] De Matos J, Britto Jr A d S, Oliveira L E, et al. Histopathologic image processing: A review[A]. 2019.
- [8] Gurcan M N, Boucheron L E, Can A, et al. Histopathological image analysis: A review[J]. *IEEE reviews in biomedical engineering*, 2009, 2: 147-171.
- [9] Li C, Xue D, Hu Z, et al. A survey for breast histopathology image analysis using classical and deep neural networks[C]//International Conference on Information Technologies in Biomedicine. Springer, 2019: 222-233.
- [10] Ghosh P, Antani S, Long L R, et al. Review of medical image retrieval systems and future directions[C/OL]//2011 24th International Symposium on Computer-Based Medical Systems (CBMS). 2011: 1-6. DOI: 10.1109/CBMS.2011.5999142.
- [11] Rahaman M M, (corresponding author) C L, Yao Y, et al. Identification of COVID-19 Samples from Chest X-Ray Images Using Deep Learning: A Comparison of Transfer Learning Approaches[J]. *Journal of X-Ray Science and Technology*, 2020, 28(5): 821-839.
- [12] Zhou X, Li C, Rahaman M M, et al. A comprehensive review for breast histopathology image analysis using classical and deep neural networks[J]. *IEEE Access*, 2020, 8: 90931-90956.
- [13] Sung H, Ferlay J, Siegel R L, et al. Global cancer statistics 2020: Globocan estimates of incidence and mortality worldwide for 36 cancers in 185 countries[J]. *CA: a cancer journal for clinicians*, 2021, 71(3): 209-249.
- [14] Renehan A G, Tyson M, Egger M, et al. Body-mass index and incidence of cancer: a systematic review and meta-analysis of prospective observational studies[J]. *The lancet*, 2008, 371(9612): 569-578.
- [15] McTiernan A, Kooperberg C, White E, et al. Recreational physical activity and the risk of breast cancer in postmenopausal women: the women's health initiative cohort study[J]. *Jama*, 2003, 290(10): 1331-1336.
- [16] Levine M E, Suarez J A, Brandhorst S, et al. Low protein intake is associated with a major reduction in igf-1, cancer, and overall mortality in the 65 and younger but not older population[J]. *Cell metabolism*, 2014, 19(3): 407-417.
- [17] on Hormonal Factors in Breast Cancer C G, et al. Alcohol, tobacco and breast cancer—collaborative reanalysis of individual data from 53 epidemiological studies, including 58 515 women with breast cancer and 95 067 women without the disease[J]. *British journal of cancer*, 2002, 87(11): 1234.
- [18] of Health U D, Services H, et al. The health consequences of smoking-50 years of progress: a report of the surgeon general[M]. Atlanta, GA: US Department of Health and Human Services, Centers for Disease, 2014.
- [19] Hunter D J, Colditz G A, Hankinson S E, et al. Oral contraceptive use and breast cancer: a prospective study of young women[J]. *Cancer Epidemiology and Prevention Biomarkers*, 2010, 19(10): 2496-2502.
- [20] Coşkun M, Uçar A, Yildirim Ö, et al. Face recognition based on convolutional neural network[C]//2017 International Conference on Modern Electrical and Energy Systems (MEES). IEEE, 2017: 376-379.
- [21] Gao H, Cheng B, Wang J, et al. Object classification using cnn-based fusion of vision and lidar in autonomous vehicle environment[J/OL]. *IEEE Transactions on Industrial Informatics*, 2018, 14(9): 4224-4231. DOI: 10.1109/TII.2018.2822828.
- [22] Monshi M M A, Poon J, Chung V, et al. Covidxraynet: Optimizing data augmentation and cnn hyperparameters for improved covid-19 detection from cxr[J/OL]. *Computers in Biology and Medicine*, 2021, 133: 104375. DOI: <https://doi.org/10.1016/j.combiomed.2021.104375>.
- [23] LeCun Y, Bottou L, Bengio Y, et al. Gradient-based learning applied to document recognition[J]. *Proceedings of the IEEE*, 1998, 86(11): 2278-2324.
- [24] Simonyan K, Zisserman A. Very deep convolutional networks for large-scale image recognition[A]. 2014.
- [25] Russakovsky O, Deng J, Su H, et al. Imagenet large scale visual recognition challenge[J]. *International journal of computer vision*, 2015, 115(3): 211-252.
- [26] Szegedy C, Liu W, Jia Y, et al. Going deeper with convolutions[C]//Proceedings of the IEEE conference on computer vision and pattern recognition. 2015: 1-9.
- [27] Chollet F. Xception: Deep learning with depthwise separable convolutions[C]//Proceedings of the IEEE conference on computer vision and pattern recognition. 2017: 1251-1258.
- [28] He K, Zhang X, Ren S, et al. Deep residual learning for image recognition[C]//Proceedings of the IEEE conference on computer vision and pattern recognition. 2016: 770-778.
- [29] Huang G, Liu Z, Van Der Maaten L, et al. Densely connected convolutional networks[C]//Proceedings of the IEEE conference on computer vision and pattern recognition. 2017: 4700-4708.
- [30] Cao Y, Geddes T A, Yang J, et al. Ensemble deep learning in bioinformatics[J]. *Nature Machine Intelligence*, 2020, 2(9): 1-9.
- [31] Yang Y, Lv H. Discussion of ensemble learning under the era of deep learning[J/OL]. *CoRR*, 2021, abs/2101.08387. <https://arxiv.org/abs/2101.08387>.
- [32] Petushi S, Garcia F U, Haber M M, et al. Large-scale computations on histology images reveal grade-differentiating parameters for breast cancer[J]. *BMC medical imaging*, 2006, 6(1): 1-11.
- [33] Singh S, Gupta P, Sharma M K. Breast cancer detection and classification of histopathological images[J]. *International Journal of Engineering Science and Technology*, 2010, 3(5): 4228.
- [34] Zhang Y, Zhang B, Lu W. Breast cancer classification from histological images with multiple features and random subspace classifier ensemble[C]//AIP Conference Proceedings: volume 1371. American Institute of Physics, 2011: 19-28.
- [35] Zhang Y, Zhang B, Coenen F, et al. Breast cancer diagnosis from biopsy images with highly reliable random subspace classifier ensembles[J]. *Machine vision and applications*, 2013, 24(7): 1405-1420.

- [36] Zhang Y, Zhang B, Lu W. Breast cancer histological image classification with multiple features and random subspace classifier ensemble [M]//Knowledge-Based Systems in Biomedicine and Computational Life Science. Springer, 2013: 27-42.
- [37] Shukla K, Tiwari A, Sharma S, et al. Classification of histopathological images of breast cancerous and non cancerous cells based on morphological features[J]. Biomedical and Pharmacology Journal, 2017, 10(1): 353-366.
- [38] Das K, Karri S P K, Roy A G, et al. Classifying histopathology whole-slides using fusion of decisions from deep convolutional network on a collection of random multi-views at multi-magnification[C]//2017 IEEE 14th International Symposium on Biomedical Imaging (ISBI 2017). IEEE, 2017: 1024-1027.
- [39] Gour M, Jain S, Sunil Kumar T. Residual learning based cnn for breast cancer histopathological image classification[J]. International Journal of Imaging Systems and Technology, 2020, 30(3): 621-635.
- [40] Breiman L. Random forests[J]. Machine learning, 2001, 45(1): 5-32.
- [41] Yan R, Ren F, Wang Z, et al. Breast cancer histopathological image classification using a hybrid deep neural network[J]. Methods, 2020, 173: 52-60.
- [42] Schuster M, Paliwal K K. Bidirectional recurrent neural networks[J]. IEEE transactions on Signal Processing, 1997, 45(11): 2673-2681.
- [43] Kausar T, Wang M, Idrees M, et al. Hwcdnn: Multi-class recognition in breast histopathology with haar wavelet decomposed image based convolution neural network[J]. Biocybernetics and Biomedical Engineering, 2019, 39(4): 967-982.
- [44] Li Y, Wu J, Wu Q. Classification of breast cancer histology images using multi-size and discriminative patches based on deep learning[J]. IEEE Access, 2019, 7: 21400-21408.
- [45] Wang Z, Dong N, Dai W, et al. Classification of breast cancer histopathological images using convolutional neural networks with hierarchical loss and global pooling[C]//International Conference Image Analysis and Recognition. Springer, 2018: 745-753.
- [46] Kassani S H, Kassani P H, Wesolowski M J, et al. Classification of histopathological biopsy images using ensemble of deep learning networks [A]. 2019. arXiv: 1909.11870.
- [47] Yang Z, Ran L, Zhang S, et al. Ems-net: Ensemble of multiscale convolutional neural networks for classification of breast cancer histology images[J/OL]. Neurocomputing, 2019, 366: 46-53. <https://www.sciencedirect.com/science/article/pii/S0925231219310872>. DOI: <https://doi.org/10.1016/j.neucom.2019.07.080>.
- [48] Anda J. Histopathology image classification using an ensemble of deep learning models[J/OL]. Sensors, 2020, 20. DOI: 10.3390/s20164373.
- [49] Senousy Z, Abdelsamea M, Gaber M M, et al. Mcua: Multi-level context and uncertainty aware dynamic deep ensemble for breast cancer histology image classification[J/OL]. IEEE Transactions on Biomedical Engineering, 2021. <http://dx.doi.org/10.1109/TBME.2021.3107446>. DOI: 10.1109/tbme.2021.3107446.
- [50] Senousy Z, Abdelsamea M, Mostafa Mohamed M, et al. 3e-net: Entropy-based elastic ensemble of deep convolutional neural networks for grading of invasive breast carcinoma histopathological microscopic images[J/OL]. Entropy, 2021, 23. DOI: 10.3390/e23050620.
- [51] Zhu C, Tao S, Chen H, et al. Hybrid model enabling highly efficient follicular segmentation in thyroid cytopathological whole slide image [J]. Intelligent Medicine, 2021, 1(2): 70-79.
- [52] Song Y, Chang H, Gao Y, et al. Feature learning with component selective encoding for histopathology image classification[C/OL]//2018 IEEE 15th International Symposium on Biomedical Imaging (ISBI 2018). 2018: 257-260. DOI: 10.1109/ISBI.2018.8363568.
- [53] Li J, Zhang J, Sun Q, et al. Breast cancer histopathological image classification based on deep second-order pooling network[C/OL]//2020 International Joint Conference on Neural Networks (IJCNN). 2020: 1-7. DOI: 10.1109/IJCNN48605.2020.9207604.
- [54] Hu C, Sun X, Yuan Z, et al. Classification of breast cancer histopathological image with deep residual learning[J]. International Journal of Imaging Systems and Technology, 2021, 31(3): 1583-1594.
- [55] Ribani R, Marengoni M. A survey of transfer learning for convolutional neural networks[C]//2019 32nd SIBGRAPI Conference on Graphics, Patterns and Images Tutorials (SIBGRAPI-T). IEEE, 2019: 47-57.
- [56] Shoeleh F, Asadpour M. Graph based skill acquisition and transfer learning for continuous reinforcement learning domains[J]. Pattern Recognition Letters, 2017, 87: 104-116.
- [57] Hadad O, Bakalo R, Ben-Ari R, et al. Classification of breast lesions using cross-modal deep learning[C]//2017 IEEE 14th International Symposium on Biomedical Imaging (ISBI 2017). IEEE, 2017: 109-112.
- [58] Sarkar D, Bali R, Ghosh T. Hands-on transfer learning with python: Implement advanced deep learning and neural network models using tensorflow and keras[M]. Packt Publishing Ltd, 2018.
- [59] Hadad O, Ran B, Ben-Ari R, et al. Ensemble learning[C]//Encyclopedia of biometrics. 2009: 270-273.
- [60] Yang A Y, Lv B H, Chen C N, et al. Ftbme: feature transferring based multi-model ensemble[J]. Multimedia Tools and Applications, 2020, 79(1).
- [61] Yang Y, Lv H, Chen N, et al. Local minima found in the subparameter space can be effective for ensembles of deep convolutional neural networks[J/OL]. Pattern Recognition, 2021, 109: 107582. DOI: <https://doi.org/10.1016/j.patcog.2020.107582>.
- [62] Li F, Yang Y, Wei Y, et al. Deep learning-based predictive biomarker of pathological complete response to neoadjuvant chemotherapy from histological images in breast cancer[J]. Journal of translational medicine, 2021, 19(1): 1-13.
- [63] Spanhol F A, Oliveira L S, Petitjean C, et al. A dataset for breast cancer histopathological image classification[J]. Ieee transactions on biomedical engineering, 2015, 63(7): 1455-1462.
- [64] Li C, Zhang J, Zhang H, et al. Generative adversarial networks based pathological images classification of poorly differentiated cervical cancer[J]. Journal of Northeastern University (Natural Science), 2020, 41(7): 1054.
- [65] Srinivas A, Lin T Y, Parmar N, et al. Bottleneck transformers for visual recognition[C]//Proceedings of the IEEE/CVF Conference on Computer Vision and Pattern Recognition. 2021: 16519-16529.
- [66] Touvron H, Cord M, Sablayrolles A, et al. Going deeper with image transformers[C]//Proceedings of the IEEE/CVF International Conference on Computer Vision. 2021: 32-42.
- [67] Xu W, Xu Y, Chang T, et al. Co-scale conv-attentional image transformers[A]. 2021.
- [68] Touvron H, Cord M, Douze M, et al. Training data-efficient image transformers & distillation through attention[C]//International Conference on Machine Learning. PMLR, 2021: 10347-10357.
- [69] Graham B, El-Nouby A, Touvron H, et al. Levit: a vision transformer in convnet's clothing for faster inference[C]//Proceedings of the

- IEEE/CVF International Conference on Computer Vision. 2021: 12259-12269.
- [70] Dosovitskiy A, Beyer L, Kolesnikov A, et al. An image is worth 16x16 words: Transformers for image recognition at scale[A]. 2020.
- [71] Yuan L, Chen Y, Wang T, et al. Tokens-to-token vit: Training vision transformers from scratch on imagenet[C]//Proceedings of the IEEE/CVF International Conference on Computer Vision. 2021: 558-567.
- [72] Tolstikhin I O, Houlsby N, Kolesnikov A, et al. Mlp-mixer: An all-mlp architecture for vision[J]. *Advances in Neural Information Processing Systems*, 2021, 34.
- [73] Liu H, Dai Z, So D, et al. Pay attention to mlps[J]. *Advances in Neural Information Processing Systems*, 2021, 34.
- [74] Touvron H, Bojanowski P, Caron M, et al. Resmlp: Feedforward networks for image classification with data-efficient training[A]. 2021.
- [75] Bayramoglu N, Kannala J, Heikkilä J. Deep learning for magnification independent breast cancer histopathology image classification[C/OL]//2016 23rd International conference on pattern recognition (ICPR). IEEE, 2016: 2440-2445. DOI: 10.1109/ICPR.2016.7900002.
- [76] Spanhol F A, Oliveira L S, Petitjean C, et al. Breast cancer histopathological image classification using convolutional neural networks[C/OL]//2016 international joint conference on neural networks (IJCNN). IEEE, 2016: 2560-2567. DOI: 10.1109/IJCNN.2016.7727519.
- [77] Spanhol F A, Oliveira L S, Cavalin P R, et al. Deep features for breast cancer histopathological image classification[C/OL]//2017 IEEE International Conference on Systems, Man, and Cybernetics (SMC). IEEE, 2017: 1868-1873. DOI: 10.1109/SMC.2017.8122889.
- [78] Song Y, Zou J J, Chang H, et al. Adapting fisher vectors for histopathology image classification[C/OL]//2017 IEEE 14th International Symposium on Biomedical Imaging (ISBI 2017). IEEE, 2017: 600-603. DOI: 10.1109/ISBI.2017.7950592.
- [79] Zhi W, Yueng H W F, Chen Z, et al. Using transfer learning with convolutional neural networks to diagnose breast cancer from histopathological images[C]//International Conference on Neural Information Processing. Springer, 2017: 669-676.
- [80] Nejad E M, Affendey L S, Latip R B, et al. Classification of histopathology images of breast into benign and malignant using a single-layer convolutional neural network[C]//Proceedings of the International Conference on Imaging, Signal Processing and Communication. 2017: 50-53.
- [81] Han Z, Wei B, Zheng Y, et al. Breast cancer multi-classification from histopathological images with structured deep learning model[J]. *Scientific reports*, 2017, 7(1): 1-10.
- [82] Wei B, Han Z, He X, et al. Deep learning model based breast cancer histopathological image classification[C]//2017 IEEE 2nd international conference on cloud computing and big data analysis (ICCCBDA). IEEE, 2017: 348-353.
- [83] Shallu, Mehra R. Breast cancer histology images classification: Training from scratch or transfer learning?[J/OL]. *ICT Express*, 2018, 4(4): 247-254. <https://www.sciencedirect.com/science/article/pii/S2405959518304934>. DOI: <https://doi.org/10.1016/j.ict.2018.10.007>.
- [84] Nahid A A, Mehrabi M A, Kong Y. Histopathological breast cancer image classification by deep neural network techniques guided by local clustering[J]. *BioMed research international*, 2018, 2018.
- [85] Nahid A A, Kong Y. Histopathological breast-image classification using local and frequency domains by convolutional neural network[J]. *Information*, 2018, 9(1): 19.
- [86] Du B, Qi Q, Zheng H, et al. Breast cancer histopathological image classification via deep active learning and confidence boosting[C]//International Conference on Artificial Neural Networks. Springer, 2018: 109-116.
- [87] Nawaz M, Sewissy A A, Soliman T H A. Multi-class breast cancer classification using deep learning convolutional neural network[J]. *Int. J. Adv. Comput. Sci. Appl*, 2018, 9(6): 316-332.
- [88] Gandomkar Z, Brennan P C, Mello-Thoms C. A framework for distinguishing benign from malignant breast histopathological images using deep residual networks[C]//14th International Workshop on Breast Imaging (IWBI 2018): volume 10718. International Society for Optics and Photonics, 2018: 107180U.
- [89] Cascianelli S, Bello-Cerezo R, Bianconi F, et al. Dimensionality reduction strategies for cnn-based classification of histopathological images [C]//International conference on intelligent interactive multimedia systems and services. Springer, 2018: 21-30.
- [90] Xu B, Liu J, Hou X, et al. Look, investigate, and classify: a deep hybrid attention method for breast cancer classification[C]//2019 IEEE 16th international symposium on biomedical imaging (ISBI 2019). IEEE, 2019: 914-918.
- [91] Bhuiyan M N Q, Shamsujjoha M, Ripon S H, et al. Transfer learning and supervised classifier based prediction model for breast cancer[M]//Big Data Analytics for Intelligent Healthcare Management. Elsevier, 2019: 59-86.
- [92] Xie J, Liu R, Luttrell IV J, et al. Deep learning based analysis of histopathological images of breast cancer[J/OL]. *Frontiers in genetics*, 2019, 10: 80. <https://www.frontiersin.org/article/10.3389/fgene.2019.00080>.
- [93] Thuy M B H, Hoang V T. Fusing of deep learning, transfer learning and gan for breast cancer histopathological image classification[C]//International Conference on Computer Science, Applied Mathematics and Applications. Springer, 2019: 255-266.